

INTERFACE WAVES ALONG FRACTURES IN ANISOTROPIC MEDIA

SIYI SHAO*, BRADLEY C. ABELL†, AND LAURA J. PYRAK-NOLTE‡

Abstract. The detection of fractures in an anisotropic medium is complicated by discrete modes that are guided or confined by layers, as well as by fractures, and that travel with velocities close ($\sim 92\%$) to the shear wave velocity. For instance, fractures can “mask” the presence of textural anisotropy in a rock, and can change the apparent shear wave velocity anisotropy. In this study, we examine the effect of fracture interface waves on the interpretation of shear wave velocities for two orthogonal polarizations propagating through a layered medium with fractures. These experimental results demonstrate that competing textural and structural properties can affect the interpretation of rock properties from seismic data. Interpretation in the presence of fractures in isotropic or anisotropic media can be unambiguously interpreted if measurements are made as a function of stress, which eliminates many fracture-generated discrete modes.

1. Introduction. Fractures in hydrocarbon reservoirs can affect the hydraulic properties of the reservoir. For instance, high-fracture density can provide high permeability, and the orientation of the fractures may determine the permeability anisotropy in the reservoir. Experimental, theoretical and computational research has been performed on seismic wave propagation in fractured media to determine the orientation of the fractures [1, 2].

However, much of the research has focused on fractured isotropic media, i.e. fractures in an isotropic matrix. Over the last decade, researchers have made much theoretical progress in studying fractures in anisotropic media. For example, Schoenberg and Sayers derived theoretically a second rank tensor for each set of fracture from a compliance tensor of transversely isotropic medium with a set of fractures and layers [3]. Diner applied the method by Schoenberg and obtained the fracture and background medium parameters from a monoclinic compliance tensor [4].

But experimental detection of fractures in an anisotropic medium is complicated because of competing attenuation mechanisms caused by layers and fractures. Both fractures and layers give rise to anisotropic shear wave velocity and to guided or confined modes depending on the wavelength relative to layer spacing or fracture specific stiffness. To solve theoretically the problem, Schoenberg (1980) proposed linear slip theory that represents fractures and other non-welded interfaces by boundary condition between two elastic medium where the stress is continuous, but the displacements are discontinuous [5]. The discontinuity in displacement is inversely proportional to the specific of the fracture [6]. Pyrak-Nolte et al. (1987) used the displacement discontinuity boundary conditions to theoretically explore the existence of fracture interface waves, i.e., coupled Rayleigh waves [7]. When two fracture surfaces are not in contact, each surface can support a Rayleigh wave. As the surfaces are brought into contact, the Rayleigh waves from each surface couple through the contact area of the fracture. It has been shown theoretically, numerically and experimentally that two interface waves exist, a slow (anti-symmetric) interface wave that depends only on the shear stiffness of the fracture and a fast (symmetric) interface wave that depends only on the normal stiffness of the fracture [7, 8, 9].

In this study, we investigated the effect of an anisotropic matrix on the existence of interface waves.

2. Experimental Setup. Experiments were performed on cubic samples (size: $\sim 100mm \times 100mm \times 100mm$) of garolite, a high performance fiber glass composite, to determine the effect of matrix anisotropy on the existence and velocity of interface waves, as well as the interpretation of seismic anisotropy. One intact and two fractured samples were used in this study and are shown in Figure 1. The dimensions of the samples are listed in Table 2.1. The intact sample (sample name: Intact), was used as a reference sample to determine the seismic anisotropy of garolite

*Department of Physics, Purdue University, West Lafayette, IN

†Department of Physics, Purdue University, West Lafayette, IN

‡Department of Physics, Department of Earth and Atmospheric Science, and School of Civil Engineering, Purdue University, West Lafayette, IN

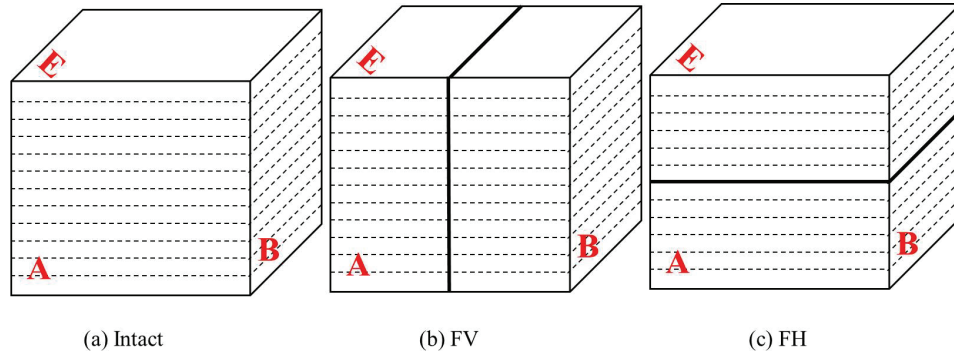


FIG. 1. A sketch of the sample used in the experiments: (a) Intact containing no through going fractures, (b) FV with a fracture perpendicular to layers, (c) FH with a fracture parallel to layers. The dashed thin lines indicate the layers, and the solid thick lines indicate the fractures in the sample. Capital letter A, B, ..., represents the face label, face C is on the opposite side of face A, face D is on the opposite side of face B, and face F is on the opposite side of face E.

TABLE 2.1
Dimensions, mass and density of samples

| Sample Name | Intact | FH | FV |
|------------------------------|---------|---------|---------|
| Dimensions (mm) | | | |
| A – C | 100.14 | 100.22 | 100.19 |
| B – D | 99.86 | 100.23 | 100.19 |
| E – F | 100.09 | 100.13 | 100.18 |
| Mass (g) | 1366.24 | 1367.81 | 1369.07 |
| Density (kg/m ³) | 1365.01 | 1359.91 | 1361.43 |

for compressional and shear waves propagated in three orthogonal directions. The fractures were created by saw cutting the samples and belt-sanding the surfaces. The difference among the fracture samples FV and FH (Figure 1b, 1c) is the orientation of the fracture relative to the layering in the matrix. The thickness of the layers in the matrix was on the order of 0.5 mm. In sample FV, the fracture was oriented perpendicular to the layering, while in sample FH, the fracture was oriented parallel to the layering. All of the samples were sealed with tape to prevent transducer couplant from penetrating into the samples during measurements.

A seismic array was used to send and receive compressional and shear waves through the samples. The position of the array relative to the loading direction is shown in Figure 2 as well as the layout of the compressional, P, and shear, S wave transducers. The seismic array consisted of a source array and a receiver array each containing two P (Olympus-Panametrics V103) and five S (Olympus-Panametrics V153) contact piezoelectric transducers with a central frequency of 1 MHz. The transducer layouts for the source and receiver arrays were mirror images of each other. The S-wave transducers were polarized either perpendicular or parallel to layers, as well as to a fracture. The transducers were coupled to a sealed sample with honey that had been baked to reduce the water content by 8.75% by weight. The couplant improves the coupling between the transducer and the machined tape-covered surface of the sample. A pulse-receiver (Panametrics 5077PR) was used to excite the source with a 0.4 microsecond duration square wave with a repetition rate of 100 Hz, amplitude of 400 V and a gain of +10 dB. The transducers and pulse-receiver were coupled through a PXI-1042 that used a PXI-5122 digitizer to record and store the full waveforms. For each transducer combination, a 100 microsecond window of the waveform with a time delay of 4 microseconds was recorded with a resolution of 0.01 microseconds/point.

The existence and velocity of interface waves depend on the stiffness of the fracture which

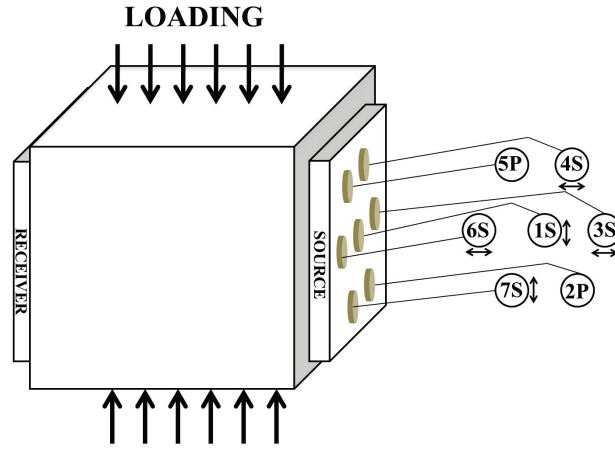


FIG. 2. The position of the source and receiver arrays relative to the direction of loading are shown as well as the location of compressional, P, and shear, S, wave transducers. The arrows next to the S-wave transducers indicate the direction of shear wave polarization.

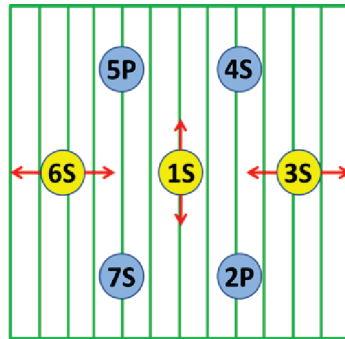


FIG. 3. Transducer layout with 1S parallel, and 3S, 6S perpendicular to layers.

increases with increasing stresses [10]. Seismic measurements were performed as a function of stress using a uniaxial loading machine (SOILTEST, Inc.) that resulted in normal stresses (normal to the sample as oriented in Figure 2) ranging from 0.4MPa to 4MPa applied in increments (either 0.08 or 0.8MPa in this study).

3. Results.

3.1. Intact Sample. Seismic wave measurements were first performed on the intact sample for two different orientations. First, waves were propagated into the page (Figure 3) that was polarized parallel to layers, while stress was applied parallel to the layers. Shear wave transducers at position 1, 3 and 6 were polarized as indicated by the red arrows in Figure 3. For the second orientation, the sample was rotated 90 degrees and the stress was applied perpendicular to layers (Figure 5).

In this paper, shear waves polarized parallel to layers are referred to as SH waves, and shear waves polarized perpendicular to layers are referred to as SV waves.

For the first sample orientation (Figure 3), 3S and 6S are SV waves, while 1S is a SH wave. In Figure 4, the SH wave arrived earlier than the SV wave, i.e., SH waves have a smaller first break delay than SV waves. Here we choose the first break delay by picking the onset time of the wave signals [1]. The results from the second sample orientation (Figure 5) for the intact sample are the same: SH waves (3S and 6S) travel faster than SV wave (1S), (Figure 6).

The shear wave velocity in the intact sample exhibits transverse isotropy (Table 3.1).

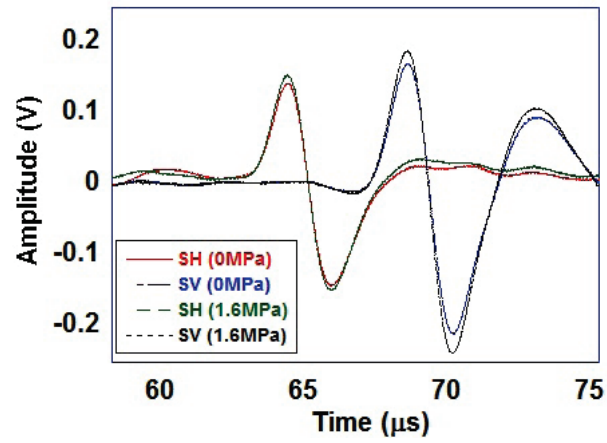


FIG. 4. Received signals for SV and SH waves on the Intact sample for applied stresses of 0 and 1.6MPa for the sample orientation shown in Figure 3.

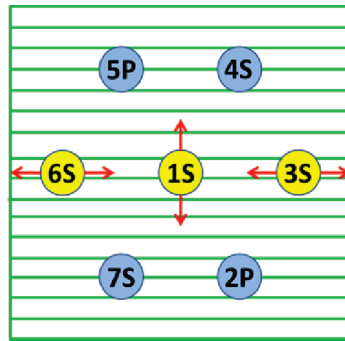


FIG. 5. Transducer layout with 1S perpendicular, 3S and 6S parallel to layers.

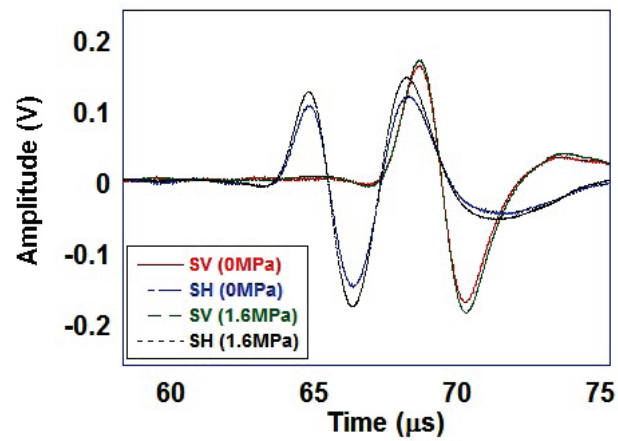


FIG. 6. Received signals for SV and SH waves on the Intact sample for applied stresses of 0 and 1.6MPa for the sample orientation shown in Figure 5.

TABLE 3.1
 First break velocities of SV and SH waves for three directions of the intact sample

| Wave direction | A-C | B-D | E-F |
|------------------------|------|------|------|
| SV wave velocity (m/s) | 1503 | 1497 | 1501 |
| SH wave velocity (m/s) | 1598 | 1601 | 1515 |

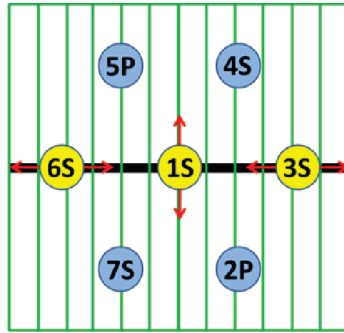


FIG. 7. A sketch of the transducer layout for sample FV with the fracture indicated by the thick black line. The red arrows give the direction of polarization of the shear waves.

3.2. Fracture Samples. We also measured shear waves propagated through fractured samples FV and FH for the same orientations and loading conditions to compare with behavior of the intact sample.

For fracture sample FV (fracture perpendicular to the layering), the transducer layout on sample surface is shown in Figure 7. 1S (SH) was polarized parallel to layers, but perpendicular to the fracture. 3S and 6S were SV waves and polarized parallel to the fracture. Signals were recorded for SH and SV waves under no stress and a stress of 1.6MPa (Figure 8).

For sample FV under low stress, the SH wave (red line in Figure 8) traveled slightly faster than SV wave (blue line in Figure 8). When the stress was increased to 1.6MPa, the SV wave (black line) didn't shift, while that of the SH wave (green line) arrived significantly earlier. The first break delay for the SH wave decreased, resulting in an increase in its first break velocity. We calculated the first break velocities for SV and SH waves by dividing the sample dimension by the first break delays, giving: 1490 m/s for SV wave under 0MPa and 1.6MPa, 1515 m/s for SH wave under 0MPa, but around 1580 m/s under 1.6MPa. We find when there's no stress, 1S wave traveled with a velocity (1515 m/s) smaller (~ 0.95) than shear wave velocity (1600 m/s), i.e. the fracture under no load supported an interface wave (Rayleigh wave), instead of a bulk shear wave.

For sample FH where the fracture is parallel to the layers, the transducer layout and polarization of the shear wave transducers are shown in Figure 9. The main difference between the transducer layout for sample FV (Figure 7) and sample FH (Figure 9) is that 1S for sample FH was SV which was perpendicular to the fracture.

We observe that waveforms of the SH wave (blue and black line in Figure 10) did not shift with change of stress, while the arrival time of the SV wave (1S in Figure 9) decreased as the stress was increased to 1.6MPa.

The SH wave velocities for FH were both around 1590 m/s at 0MPa and 1.6MPa. The SV wave velocity was 1420 m/s at 0MPa, and increased to 1500 m/s when the stress was increased to 1.6MPa. So in this case, the fracture also supported an interface wave polarized perpendicular to the fracture.

To determine the effect of stress on the first break velocities, additional experiments were performed on samples FV and FH, with same transducer configurations shown in Figure 7 & 9. In these experiments, the stress was increased in increments of 0.08MPa from 0 to 1.6MPa. The velocities as a function of stress for FV and FH are shown in Figures 11 and 12, respectively, and

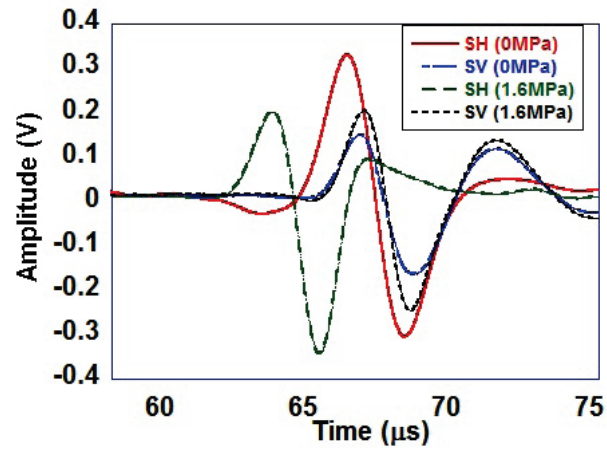


FIG. 8. Shear wave signals for SV and SH waves under 0 and 1.6MPa for fracture sample FV.

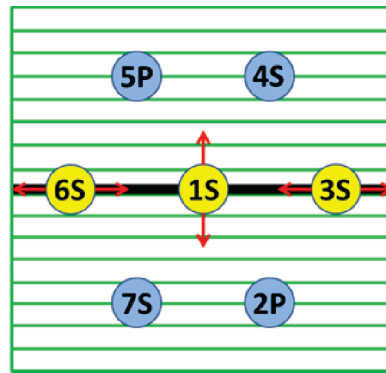


FIG. 9. A sketch of the transducer layout for sample FH with the fracture indicated by the thick black line. The red arrows give the direction of polarization of the shear waves.

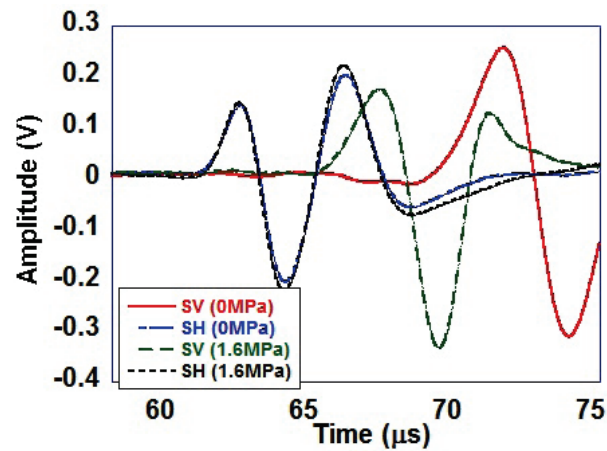


FIG. 10. Shear wave signals for SV and SH waves under 0 and 1.6MPa for fracture sample FH.

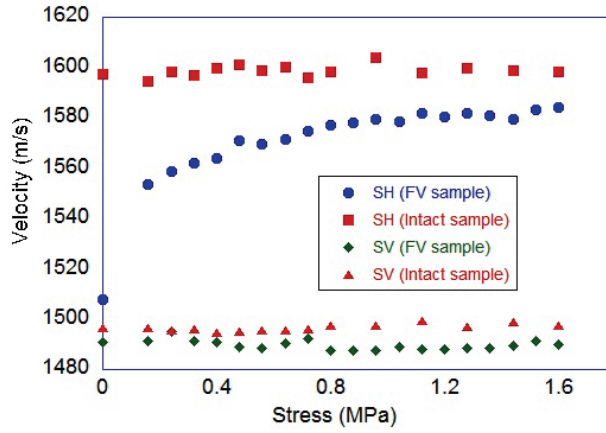


FIG. 11. SV and SH Wave velocity as a function of stress for FV and the Intact sample.

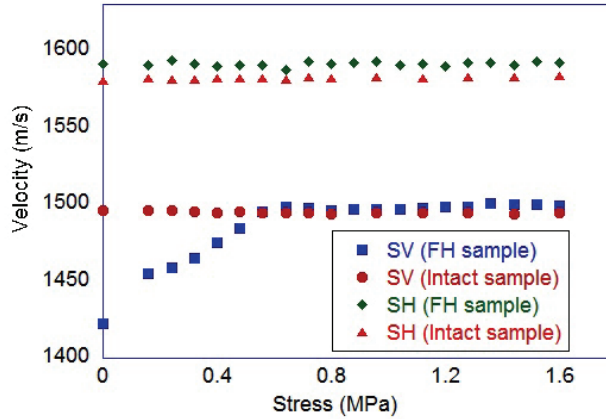


FIG. 12. SV and SH Wave velocity as a function of stress for FH and the Intact sample.

both are compared to the velocity measured for the intact sample.

From Figure 11 & 12, we find SV and SH wave velocities for the intact sample vary slightly (less than 0.2%) as the stress increased from 0 to 1.6MPa, and the shear waves parallel to the fracture (SV for FV sample, SH for FH sample) also did not change with increasing stress. However, the velocities of the shear waves polarized perpendicular to the fracture (SH for FV sample, SV for FH sample) increased with increasing stress from 0 (support interface wave) to 0.8MPa (support bulk shear wave), and then remained mostly unchanged.

4. Analysis and Discussion. We used a wavelet analysis to study the spectral content of measured shear waves. Wavelet analysis provides a direct quantitative measure of wave amplitude as functions of group delay and frequency. Four wavelet transforms are shown in Figure 13.

In the wavelets, it is observed that the dominant spectral peak decreases in arrival time with increasing stress (e.g. compare Figure 13 (a) to (b) or (c) to (d)). The frequency of the spectral peak was used to obtain the group delay at that frequency, and to calculate the corresponding group velocities.

In this study, we selected $f=0.226\text{MHz}$ to obtain the group velocities. We observed the following (Figure 14):

- (i) When the fracture was oriented perpendicularly to the layers (sample FV), for low stresses,

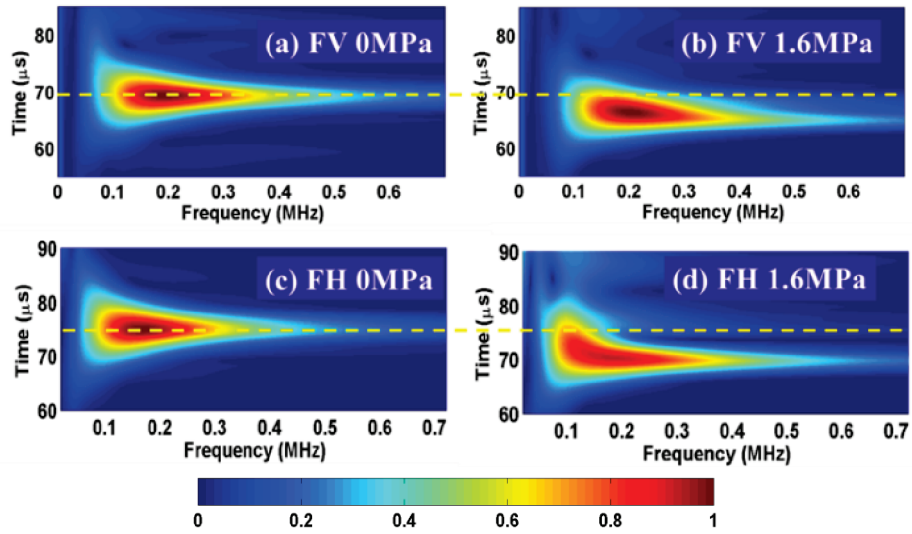


FIG. 13. Wave amplitude as functions of frequency and group delay for FV and FH sample. Color bar indicates the normalized amplitude. Yellow lines mark the average time of the peak of the signal at 0MPa.

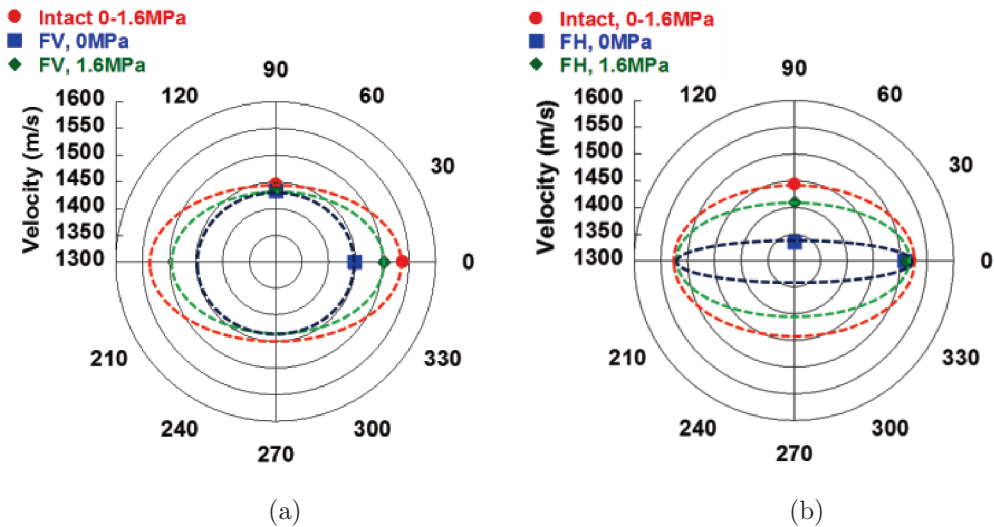


FIG. 14. Group shear wave velocities at position 1 (Figure 2b) for: (a) Intact and FV sample; (b) Intact and FH sample. Polarization direction respective to the layering are specified around the circles. The dashed ellipses are to guide the eye.

the group shear wave velocities for both polarizations were ~ 1425 m/s and ~ 1450 m/s, making the sample appear nearly isotropic. However, increasing the normal stress on the fracture increased the seismic anisotropy. When stress was increased to 1.6MPa, the interface wave velocity increased to ~ 1500 m/s, while the SH wave velocity remained ~ 1425 m/s.

(ii) When the fracture was oriented parallel to the layers, under low stress, the group shear wave velocities for both polarizations were ~ 1330 m/s and ~ 1500 m/s making the sample appear more anisotropic; but increasing the normal stress on the fracture decreased the anisotropy. When stress was increased to 1.6MPa, the interface wave velocity increased to ~ 1410 m/s, while SH wave velocity remained ~ 1500 m/s.

Interface waves were measured when the source and receiver transducers were polarized per-

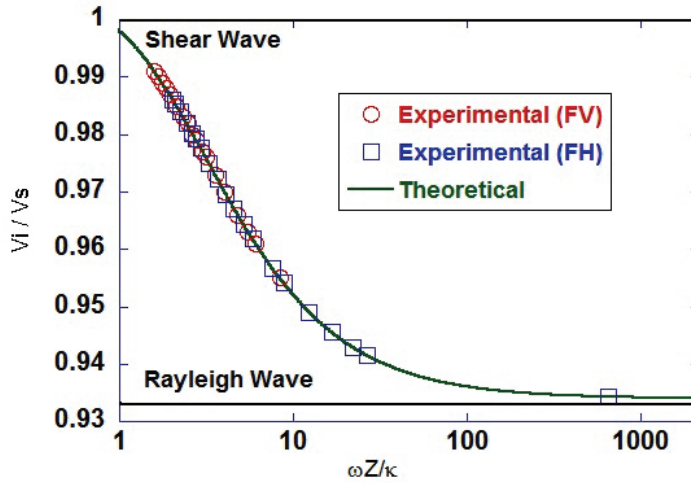


FIG. 15. Theoretical calculation and experimental data of normalized interface wave velocity as a function of normalized frequency $\omega Z/\kappa$, for sample FV and FH.

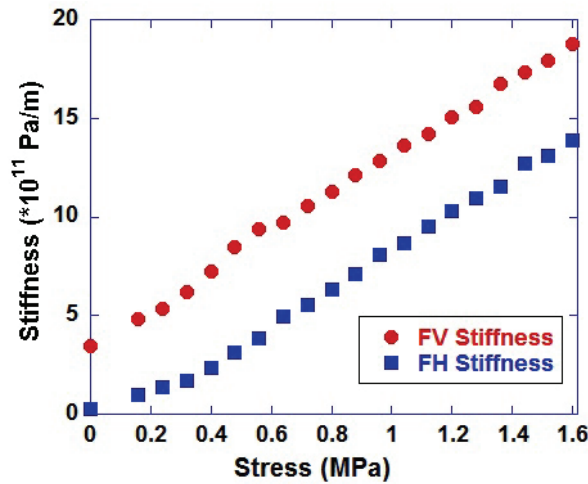


FIG. 16. Fracture specific stiffness as a function of stress, for sample FV and FH.

pendicular to a fracture. After obtaining the parameters of garolite samples, including density, group shear wave velocity and compressional wave velocity (obtained from P-style transducer at position 2 and 5 of Figure 2), we used the theory for interfaces to estimate the normalized interface wave velocity as a function of normalized frequency $\omega Z/\kappa$, (κ is the fracture specific stiffness, ω is frequency, Z =density*phase velocity), by the method provided by Pyrak-Nolte et al [7] (Figure 15). Then the experimental data were fit to the theory to estimate the specific fracture stiffness for sample FV and FH as a function of normal stress. We observe that fracture stiffness for both FV and FH appears to increase linearly with increasing stress which is an indication of low contact area (Figure 16).

5. Conclusion. In this study, we measured seismic waves propagating through three layered garolite samples, one intact, one with a fracture perpendicular to layers (sample FV), and the other with a fracture parallel to layers (sample FH). We observed that shear waves polarized parallel to layers (SH wave) traveled faster than those polarized perpendicular to layers (SV wave) of the intact

sample, which means layered garolite sample exhibits shear wave anisotropy.

The behavior of the fractured samples was different from that of the intact sample. For FV, interface waves propagated along the fracture with wave velocities closer in magnitude to SV waves than to SH waves under low stresses, making the sample appear almost isotropic. In another word, the fracture in sample FV “masked” the presence of textural anisotropy in the sample. When normal stress increased, the fractured sample exhibited shear wave velocities closer to the intact sample, giving rise to an increase of shear wave anisotropy. Sample FH exhibited the opposite trend with stress, its shear wave anisotropy decreased with increasing normal stress.

Acknowledgments. The authors wish to acknowledge support of this work by the Geosciences Research Program, Office of Basic Energy Sciences US Department of Energy (DE-FG02-09ER16022).

References.

1. Mollhoff, M., C.J. Bean, and P.G. Meredith. 2010. Rock fracture compliance derived from time delays of elastic waves. *Geophysical Prospecting*. 58: 1,111–1,121.
2. Montoya, P., W. Fisher, R. Marrett, and R. Tatham. 2002. Estimation of fracture orientation and relative intensity using azimuthal variation of P-wave AVO responses and oriented core data in the Tacata Field, Venezuela. *Society of Exploration Geophysics Annual Meeting Expanded Technical Program Abstracts with Biographies*. 72: 261–264.
3. Schoenberg, M., and C.M. Sayers. 1995. Seismic anisotropy of fractured rock. *Geophysics*. 60: 204–211.
4. Diner, C. 2011. Decomposition of compliance tensor for fractures and transversely isotropic medium. In *Proceedings of the journal Geophysical Prospecting*.
5. Schoenberg, M. 1980. Elastic wave behavior across linear slip interfaces. *J. Acoust. Soc. Am.* 68(5): 1,516–1,520.
6. Brown, S.R., and C.H. Scholz. 1985. Broad Bandwidth Study of the Topography of Natural Rock Surfaces. *J. Geophys. Res.* 90: 12,575–12,582.
7. Pyrak-Nolte, L.J., and N.G.W. Cook. 1987. Elastic interface waves along a fracture. *Geophys. Res. Lett.* 14(11): 1,107–1,110.
8. Pyrak-Nolte, L.J., J. Xu and G.M. Haley. 1992. Elastic interface waves propagating in fracture. *Phys. Rev. Lett.* 68: 3,650–3,653.
9. Gu, B., K.T. Nihei, L.R. Myer and L.J. Pyrak-Nolte. 1996. Fracture interface waves. *Journal. Geophys. Res.* 101: 827–835.
10. Pyrak-Nolte, L.J., L.R. Myer and N.G.W. Cook. 1987. Transmission of seismic waves across natural fractures. *Journal. Geophys. Res.* 95: 8,617–8,638.